

# 탄소 및 은 잉크 기반의 전위차 나트륨 이온 센서 제조 및 이의 전기화학적 특성

김서진 · 손선규 · 윤조희 · 최봉길<sup>†</sup>

강원대학교(삼척캠퍼스) 화학공학과  
(2021년 5월 31일 접수, 2021년 7월 7일 수정, 2021년 7월 12일 채택)

## Fabrication of Potentiometric Sodium-ion Sensor Based on Carbon and Silver Inks and its Electrochemical Characteristics

Seo Jin Kim, Seon Gyu Son, Jo Hee Yoon, and Bong Gill Choi<sup>†</sup>

Department of Chemical Engineering, Kangwon National University, Gangwon-do 25913, Korea  
(Received May 31, 2021; Revised July 7, 2021; Accepted July 12, 2021)

### 초 록

본 연구에서는 탄소 및 은 잉크를 사용하여 스크린 인쇄 공정을 통한 전위차 나트륨 이온( $\text{Na}^+$ ) 센서를 제작하였다. 센서의 두 전극 구성은  $\text{Na}^+$  용액에서 네른스트 거동에 따라 전극의 전위차를 발생하였다. 제조된  $\text{Na}^+$  센서는 이상적인 네른스트 민감도, 빠른 응답 시간 및 낮은 검출 한계를 보여주었다. 네른스트 반응은 센서의 반복성 및 장기 내구성 테스트 시 안정적이었다. 탄소 전극에 코팅된  $\text{Na}^+$  선택막은 간섭 이온에 대해 나트륨 이온을 선택적으로 통과시켜 우수한 선택성을 증명하였다. 휴대용  $\text{Na}^+$  센서는 인쇄 회로 시스템을 사용하여 제작되었으며 다양한 실제 샘플에서  $\text{Na}^+$  농도를 성공적으로 측정하는 것을 증명하였다.

### Abstract

A potentiometric sodium-ion ( $\text{Na}^+$ ) sensor was prepared using a screen-printing process with carbon and silver inks. The two-electrode configuration of the sensor resulted in potential differences in  $\text{Na}^+$  solutions according to Nernstian equation. The obtained  $\text{Na}^+$ -sensor exhibited an ideal Nernstian sensitivity, fast response time, and low limit of detection. The Nernstian response was stable when the sensor was tested for repeatability and long-term durability. The  $\text{Na}^+$ -selective membrane coated onto the carbon electrode selectively passed sodium ions against interfering ions, indicating an excellent selectivity. The portable  $\text{Na}^+$ -sensor was finally fabricated using a printed circuit system, demonstrating the successful measurements of  $\text{Na}^+$  concentrations in various real samples.

**Keywords:** Electrolyte ion sensor, Electrochemistry, Ink, Screen printing, Sodium

## 1. Introduction

Sodium-ion ( $\text{Na}^+$ ) is a monoatomic monocation that plays an important role in human metabolism and health. People intake  $\text{Na}^+$  from food they consume every day[1]. A small amount of  $\text{Na}^+$  (200~500 mg) is required to carry out vital functions in the human body, such as nerve impulses, muscle contraction and relaxation, and balance of water and minerals[1]. With increased production of processed food and change in lifestyles due to urbanization, salt consumption has increased to an average of 10.06 g/day (equivalent to 3.95 g sodium/day) [2]. WHO guidelines recommend a reduction in this daily salt con-

sumption, i.e., less than 5 g/day for adults[3]. Excess intake of salt in the diet leads to several health issues, such as high blood pressure, heart disease, and stroke[4]. Therefore, there is an urgent requirement for the development of a real-time monitoring system to determine the level of  $\text{Na}^+$  intake to help in maintaining human health by monitoring salt intake.

To date, several methods have been employed to detect  $\text{Na}^+$ , such as colorimetric methods, spectroscopy methods, field-effect transistor sensors, and electrochemical sensors[5-7]. Among these, electrochemical ion sensors based on ion-selective membrane electrodes provide advantages of simple maintenance, low cost, accuracy, and fast detection[8-14]. The electrochemical ion sensor consists of a two-electrode configuration with a working electrode and a reference electrode [9]. These sensors can read the change in the sodium-ion concentration when there is a change in the open-circuit potential difference between the two electrodes. The relationship between ion concentration and po-

<sup>†</sup> Corresponding Author: Kangwon National University,  
Department of Chemical Engineering, Gangwon-do 25913, Korea  
Tel: +82-33-570-6545 e-mail: bgchoi@kangwon.ac.kr

tential difference is given by the Nernstian equation[12]. Therefore, the performance of a sensor is influenced by the stability and reliability of the electrode potential.

We developed a simple, low cost, and reusable potentiometric  $\text{Na}^+$ -sensor using a screen-printing process with carbon and silver inks. Screen-printed carbon and silver inks were fabricated onto a polyethylene terephthalate (PET) substrate. The working electrode was prepared by coating a  $\text{Na}^+$ -selective membrane on a carbon conductor, while for the reference electrode,  $\text{Ag}/\text{AgCl}$  was coated onto a silver conductor. The two-electrode potentiometric  $\text{Na}^+$ -sensor exhibited high sensitivity, fast response time, good repeatability, and excellent stability over a long period of time of 15 h. Furthermore, real-time monitoring of  $\text{Na}^+$  concentration was demonstrated using wireless electronic module-integrated  $\text{Na}^+$ -sensors.

## 2. Experimental

### 2.1. Materials

Sodium ionophore X, sodium tetrakis [3,5-bis(trifluoromethyl) phenyl] borate (NaBARF), bis(2-ethylhexyl)sebacate (DOS), polyvinyl chloride (PVC), BUTVAR® B-98 (polyvinyl butyral) (PVB), tetrahydrofuran (THF), potassium chloride, calcium chloride, sodium chloride, magnesium chloride, and ammonium chloride were purchased from Sigma-Aldrich (USA). Silver (LS-405-5) and carbon pastes (FTU-16) were obtained from Asahi Chemical Research Laboratory (Japan). Deionized water (18.2 MW resistivity) was used in all experiments.

### 2.2. Preparation of screen-printed electrodes

Screen-printed electrodes of  $\text{Na}^+$ -sensor comprising carbon and silver inks were fabricated using a screen-printing system (SJ-7450S, SUNG-JIN) and a custom stainless-steel mask developed using AutoCAD software. Carbon and silver inks were screen-printed on a flexible PET substrate. The screen-printed electrodes, which comprised a working electrode (patterned with carbon paste) and a reference electrode (patterned with silver paste), were cured at 60 °C for 30 min in a convection oven.

### 2.3. Fabrication of $\text{Na}^+$ -sensor

A  $\text{Na}^+$ -selective membrane cocktail was prepared by mixing  $\text{Na}^+$  ionophore (1% w/w), NaBARF (0.55% w/w), DOS (65.45% w/w), and PVC (33% w/w) in THF (1 mL). The  $\text{Na}^+$  electrode was fabricated by drop-casting 4 mL of this cocktail on the surface of the carbon elec-

trode and left to dry overnight at room temperature. The resultant  $\text{Na}^+$  electrode was pre-conditioned by immersion in  $10^{-3}$  M NaCl for one day. The reference electrode was prepared by depositing chloride on the surface of the printed Ag electrode, followed by coating with NaCl-containing PVB[15]. The electrodeposition of chloride was performed by immersing the printed Ag electrode in 1 M KCl solution, and then, a constant potential of 0.2 V was applied to the Ag electrode for 10 min. To ensure the potential stability of the reference electrode, NaCl-containing PVB (78:50 wt% in PVB and NaCl) was coated onto the surface of this  $\text{Ag}/\text{AgCl}$  electrode.

### 2.4. Characterization

Scanning electron microscopy (SEM) images were obtained using field-emission scanning electron microscopy (FE-SEM, JSM-6701F, JEOL Ltd.). Optical microscopy (OM) images were obtained using an optical microscope (OM, BX53MTRF-S, OLYMPUS). All electrochemical characterizations were performed using a CHI760E (CH Instruments, USA) at room temperature ( $25 \pm 4$  °C), and the obtained data were within the error range of  $\pm 1\%$ . The reference electrode of  $\text{Ag}/\text{AgCl}/\text{KCl}$  (sat.) (Model K0260, AMETEK) was used for electrochemical measurements. To measure the electromotive force responses, 1 M NaCl solution was diluted from  $10^{-1}$  M to  $10^{-4}$  M NaCl solutions. The long-term stability of the  $\text{Na}^+$ -sensor was tested by immersing the sensor in  $10^{-1}$  M NaCl solution and measuring the EMF signals during 15 h. The stability was evaluated by the potential drift calculated by EMF changes between 5 and 12 h. The response time was tested by measuring the change of the EMF signals as the  $\text{Na}^+$  concentration was decreased from 100 to 1 mM NaCl solution. The response time was evaluated by the time reached to an average of the EMF signals measured in 1 mM. The real-sample test was performed using a printed circuit board (PCB) system[8].

## 3. Result and Discussion

The preparation of the  $\text{Na}^+$ -sensor using screen-printing with carbon and silver inks is schematically illustrated in Figure 1. The  $\text{Na}^+$ -sensor comprised working and reference electrodes. Carbon and silver inks were printed on a PET substrate (dimensions 35 mm  $\times$  15 mm). Carbon and silver pastes were used as conductive circuits in the working and reference electrodes, respectively, as shown in Figure 2(a) and 2(b), respectively. SEM images revealed that carbon and silver were compactly deposited on the PET surface. The  $\text{Na}^+$ -selective membrane

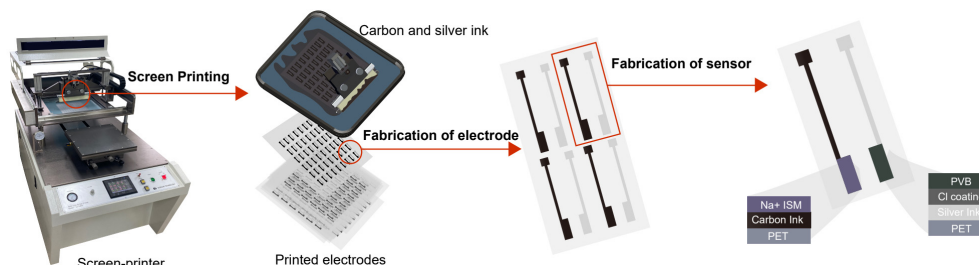


Figure 1. Schematic illustration of preparing  $\text{Na}^+$ -sensor using a screen-printing process with carbon and silver pastes.

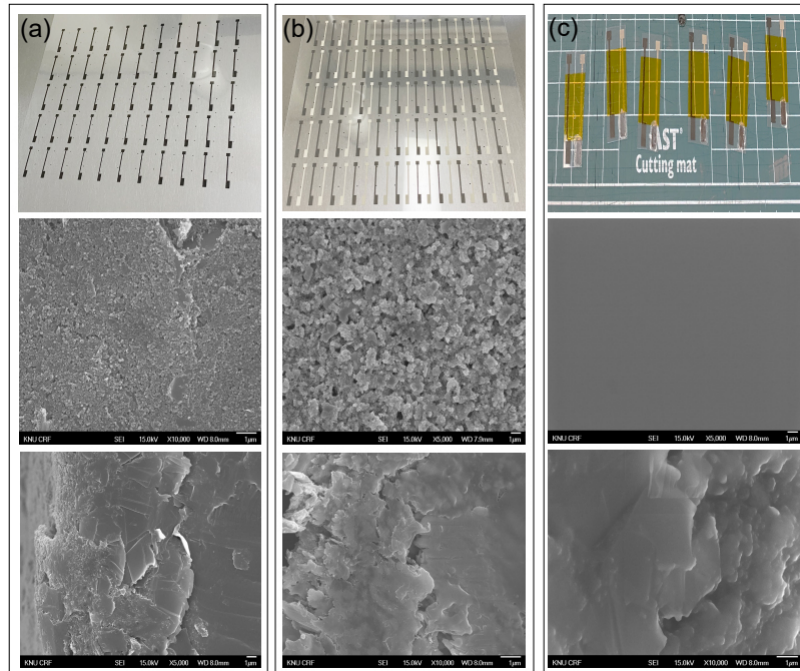


Figure 2. Photographs and SEM images of surface and cross-section of (a) carbon electrode, (b) silver electrode, and (c)  $\text{Na}^+$ -selective electrode.

was coated onto the surface of the printed carbon electrode, which was used as the working electrode [Figure 2(c)]. The reference electrode was prepared by depositing chloride ions onto the surface of the printed Ag electrode, followed by coating with NaCl-containing PVB. The  $\text{Na}^+$ -sensor collects specific sodium ions in solution samples, and then converts the activity of ions into an electrical signal. The  $\text{Na}^+$  selectively penetrates through the ion-selective membrane into the surface of carbon electrode. The moved ions are accumulated in an electrical double layer at the electrode and membrane interface. The carbon electrode serves as an ion-to-electron transducer that transduce ionic signals to electrical signals through an electrical double layer capacitance[11].

To evaluate the performance of the  $\text{Na}^+$ -sensor, electromotive force (EMF) between the working and the reference electrode was measured using a potentiometric technique. Four different  $\text{Na}^+$  concentrations were prepared: 100, 10, 1, and 0.1 mM. The  $\text{Na}^+$ -sensor was immersed in  $\text{Na}^+$  solution, and EMF signals were collected at room temperature for 30 s [Figure 3(a)]. EMF decreased linearly with the decrease in  $\text{Na}^+$  concentration. The calibration curve of EMF versus  $\log [\text{Na}^+]$  is shown in Figure 3(b). Average values were obtained from three samples of  $\text{Na}^+$ -sensors. The linear slope indicates the sensitivity of  $\text{Na}^+$ -sensors, resulting in 64.15 mV/log  $[\text{Na}^+]$  ( $R^2 = 99.88\%$ ) in a linear range of 100–0.1 mM. This indicates that the obtained  $\text{Na}^+$ -sensors show Nernstian behavior. The response time was measured according to the IUPAC recommendations[16,17]. Here, response time is defined as the time at which the initial EMF value of the  $\text{Na}^+$ -sensor reaches an average of the final value. As the  $\text{Na}^+$  concentration was decreased from 100 to 1 mM, the EMF signal decreased rapidly and stabilized [Figure 3(c)]. Based on the definition of response time, the  $\text{Na}^+$ -sensor exhibited a fast response time of  $< 5.4$  s. The limit of detection for the  $\text{Na}^+$ -sensor

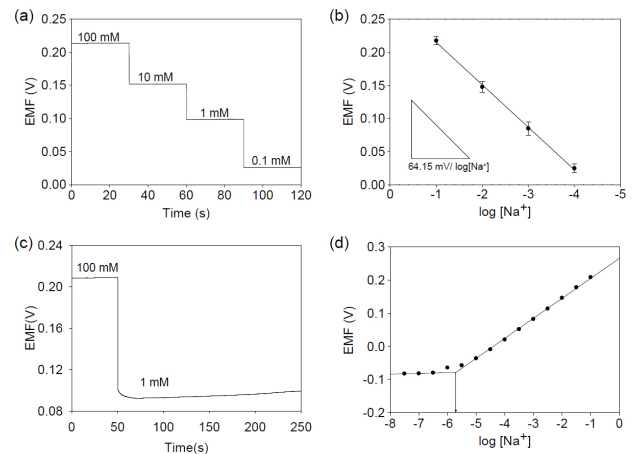
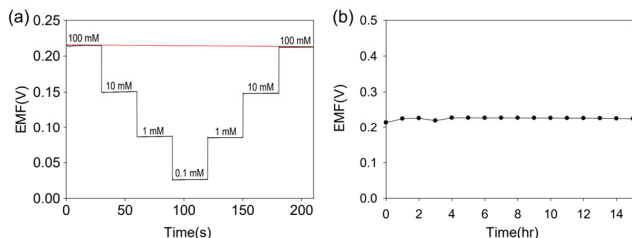


Figure 3. (a) EMF responses of  $\text{Na}^+$ -sensor with decreasing  $\text{Na}^+$  concentration. (b) Calibration curve of EMF versus  $\log [\text{Na}^+]$  for  $\text{Na}^+$ -sensor. (c) Response time test by diluting NaCl solution from 100 mM to 1 mM. (d) Limit of detection test of  $\text{Na}^+$ -sensor.

was evaluated by the intersection of the two slope lines in the calibration curve [Figure 3(d)]. As a result, the  $\text{Na}^+$ -sensor showed a low limit of detection, i.e., 0.002 mM.

To investigate the repeatability of the  $\text{Na}^+$ -sensor, the sensor was tested in  $\text{Na}^+$  solutions with concentrations decreasing from 100 to 0.1 mM [Figure 4(a)]. All initial EMF values for the  $\text{Na}^+$ -sensor were almost maintained during the repeatability test. In addition, the sensitivity for forwards and backward directions was calculated to be 62.92 and 62.24 mV/log  $[\text{Na}^+]$ , respectively. This indicates that the  $\text{Na}^+$ -sensor can be used repeatedly without significant change. The potential drift of the  $\text{Na}^+$ -sensor was tested by measuring the EMF responses at a constant



**Figure 4.** (a) Repeatability test of  $\text{Na}^+$ -sensor by measuring EMF responses in a range of 100–0.1 mM NaCl solution. (b) EMF responses of  $\text{Na}^+$ -sensor measured at a constant 100 mM NaCl concentration.

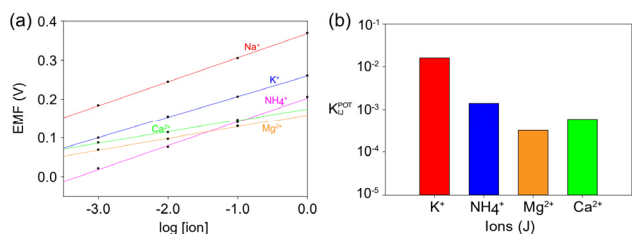


**Figure 5.** (a) EMF responses of  $\text{Na}^+$ -sensors with different ions,  $\text{NH}_4^+$ ,  $\text{K}^+$ ,  $\text{Na}^+$ ,  $\text{Ca}^{2+}$ , and  $\text{Mg}^{2+}$ . (b) Selectivity coefficients of  $\text{Na}^+$ -sensors against different ions ( $\text{NH}_4^+$ ,  $\text{K}^+$ ,  $\text{Ca}^{2+}$ , and  $\text{Mg}^{2+}$ ).

concentration of  $\text{Na}^+$  (100 mM) over a long period of 15 h [Figure 4(b)]. The potential drift was calculated by measuring the changes in EMF between 5 and 12 h. The sensor showed stable EMF responses, resulting in a low drift of 0.0467 mV/h, measured at 100 mM  $\text{Na}^+$  concentration. This value indicates that the  $\text{Na}^+$ -sensor has long-term stability for  $\text{Na}^+$  detection.

The sensor selectivity was also tested by evaluating the selectivity coefficients ( $K_{I,J}^{\text{pot}}$ ) using the IUPAC recommended separate-solution method[18,19]. EMF responses of the  $\text{Na}^+$ -sensor were measured in different interfering ion solutions, such as  $\text{K}^+$ ,  $\text{NH}_4^+$ ,  $\text{Ca}^{2+}$ , and  $\text{Mg}^{2+}$  [Figure 5(a)]. Based on the  $N$  values, the  $K_{I,J}^{\text{pot}} < 1$  indicates good selectivity of the sensors against interfering ions. As shown in Table 1, all  $K_{I,J}^{\text{pot}}$  values for the  $\text{Na}^+$ -sensor were  $< 1$ . This indicates that the  $\text{Na}^+$ -sensor could accurately measure  $\text{Na}^+$  concentration in the presence of interfering cations. Potentiometric selectivity coefficients were calculated using the separate-solution method to investigate selectivity of the  $\text{Na}^+$ -sensor. The potentiometric responses were recorded in different interfering ion solutions at a concentration of 0.1 mM. The selectivity coefficient ( $K$ ) is expressed as follows[19].

$$\Delta E = E_J - E_I = \frac{RT}{zF} \ln 10 \left\{ \frac{z_I - z_J}{z_J} \log C + \log K_{I,J}^{\text{pot}} \right\} \quad (1)$$

where  $K_{I,J}^{\text{pot}}$  is the selectivity coefficient,  $I$  is the primary ion, and  $J$  is the interfering ion. Figure 5(b) shows  $K_{I,J}^{\text{pot}}$  values for  $\text{Na}^+$ -sensors against various interfering cations of  $\text{MgCl}_2$ ,  $\text{CaCl}_2$ ,  $\text{NH}_4\text{Cl}$ , and  $\text{KCl}$ . IUPAC describes that  $K_{I,J}^{\text{pot}} < 1$  indicates good selectivity of ion-selective sensors in the presence of interfering cations. Based on  $K_{I,J}^{\text{pot}}$  values  $< 1$ ,  $\text{Na}^+$ -sensors exhibited excellent selectivity.

**Table 1.** Selectivity Coefficients of the  $\text{Na}^+$ -sensor Using a SSM with the Interference Ions of  $\text{K}^+$ ,  $\text{NH}_4^+$ ,  $\text{Ca}^{2+}$ , and  $\text{Mg}^{2+}$ .

Ions (J)	$\log K_{I,J}^{\text{pot}}$	$K_{I,J}^{\text{pot}}$
$\text{K}^+$	-1.795	$1.60 \times 10^{-2}$
$\text{NH}_4^+$	-2.855	$1.40 \times 10^{-3}$
$\text{Ca}^{2+}$	-3.499	$3.17 \times 10^{-4}$
$\text{Mg}^{2+}$	-3.230	$5.89 \times 10^{-4}$

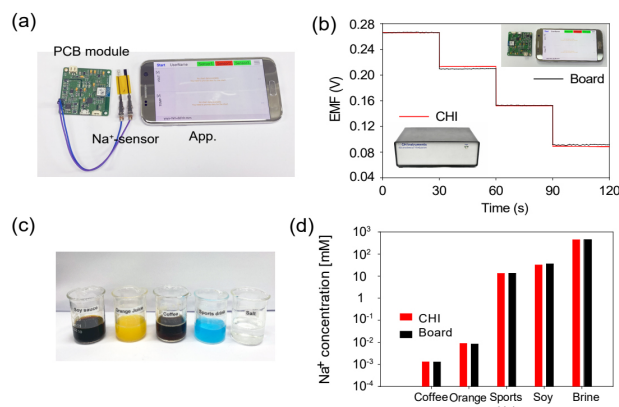


**Figure 6.** (a) Photograph of  $\text{Na}^+$ -sensor integrated with a PCB module and mobile application. (b) EMF responses of  $\text{Na}^+$ -sensor using an electrochemical instrument (CHI 760E) and wireless electronic module. (c) Photograph of real samples for coffee, orange juice, sports drink, soy sauce, and brine. (d)  $\text{Na}^+$  concentrations of real samples measured by the  $\text{Na}^+$ -sensor using an electrochemical instrument (CHI 760E) and a wireless electronic module.

To demonstrate the potential of the  $\text{Na}^+$ -sensor in point-of-care applications, a prototype of a portable  $\text{Na}^+$ -sensor was prepared by integrating it with a wireless electronic module. A PCB system is shown in Figure 6(a). It involves potentiometric ion sensors, interface circuits, a microcontroller, an analog-to-digital converter, and a communication module based on Bluetooth low energy. The PCB collects EMF signals from the  $\text{Na}^+$ -sensor, and the data are transferred to a mobile application. The portable  $\text{Na}^+$ -sensor exhibited a high sensitivity of 58.25 mV/log  $[\text{Na}^+]$  according to different concentrations of  $\text{Na}^+$  solutions [Figure 6(b)]. This value is consistent with that of the  $\text{Na}^+$ -sensor measured with an electrochemical analyzer (CHI 760E). The real-sample test of the PCB-based  $\text{Na}^+$ -sensor was performed using various samples of coffee, sports drink, orange juice, soy sauce, and brine [Figure 6(c) and (d)]. The results of the PCB-based  $\text{Na}^+$ -sensor were compared with those of a commercial  $\text{Na}^+$  electrochemical analyzer (CHI 760E). The obtained values were almost similar, with small variations. Notably, the PCB-based  $\text{Na}^+$ -sensor could accurately measure  $\text{Na}^+$  concentration in different types of real samples.

## 4. Conclusion

Potentiometric  $\text{Na}^+$ -sensors were fabricated using a screen-printing process with carbon and silver pastes. The two-electrode configuration

enabled accurate measurement of Na<sup>+</sup> concentration according to Nernstian behavior. The Na<sup>+</sup>-sensors showed a high sensitivity of 64.15 mV/log [Na<sup>+</sup>], a low detection limit of 0.002 mM, and a fast response time of < 5.4 s. The sensitivity was maintained during two-cycle tests. In addition, the potentiometric response was maintained over a long period of 15 h. The selectivity test resulted in good selectivity of Na<sup>+</sup>-sensors against interfering ions. A prototype of the portable Na<sup>+</sup>-sensor was fabricated using a PCB system. This portable Na<sup>+</sup>-sensor accurately measured the sodium-ion concentration in various real samples.

## References

1. N. J. Aburto, A. Ziolkovska, L. Hooper, P. Elliott, F. P. Cappuccio, J. J. Meerpohl, Effect of lower sodium intake on health: systematic review and meta-analyses, *BMJ*, **346**, f1326 (2013).
2. J. Powles, S. Fahimi, R. Micha, S. Khatibzadeh, P. Shi, M. Ezzati, R. E. Engell, S. S. Lim, G. Danaei, D. Mozaffarian, Global, regional and national sodium intakes in 1990 and 2010: a systematic analysis of 24 h urinary sodium excretion and dietary surveys worldwide, *BMJ Open*, **3**, e003733 (2013).
3. WHO, Guideline: Sodium intake for adults and children, World Health Organization (WHO), Geneva (2012).
4. P. Strazzullo, L. D'Elia, N.-B. Kandala, F. P. Cappuccio, Salt intake, stroke, and cardiovascular disease: meta-analysis of prospective studies, *BMJ*, **339**, b4567 (2009).
5. P. Traiwatcharanon, W. Siriwatcharapiboon, and C. Wongchoosuk, Electrochemical Sodium Ion Sensor Based on Silver Nanoparticles/Graphene Oxide Nanocomposite for Food Application, *Chemosensors*, **8**, 58 (2020).
6. A. J. Bandodkar, D. Molinnus, O. Mirza, T. Guinovart, J. R. Windmiller, G. Valdés-Ramírez, F. J. Andrade, M. J. Schöning, J. Wang, Epidermal tattoo potentiometric sodium sensors with wireless signal transduction for continuous non-invasive sweat monitoring, *Biosens. Bioelectron.*, **54**, 603-609 (2014).
7. M. Parrilla, J. Ferré, T. Guinovart, and F. J. Andrade, Wearable Potentiometric Sensors Based on Commercial Carbon Fibres for Monitoring Sodium in Sweat, *Electroanalysis*, **28**, 1267-1275 (2016).
8. J. H. Yoon, S.-M. Kim, H. J. Park, Y. K. Kim, D. X. Oh, H.-W. Cho, K. G. Lee, S. Y. Hwang, J. Park, B. G. Choi, Highly self-healable and flexible cable-type pH sensors for real-time monitoring of human fluids, *Biosens. Bioelectron.*, **150**, 111946 (2020).
9. M. Parrilla, M. Cuartero, G. A. Crespo, Wearable potentiometric ion sensors, *Trends Anal. Chem.*, **110**, 303-320 (2019).
10. J. Bobacka, A. Ivaska, and A. Lewenstam, Potentiometric Ion Sensors, *Chem. Rev.*, **108**, 329-351 (2008).
11. A. Bratov, N. Abramova, A. Ipatov, Recent trends in potentiometric sensor arrays-A review, *Anal. Chim. Acta*, **678**, 149-159 (2010).
12. E. Zdrachek, and E. Bakker, Potentiometric Sensing, *Anal. Chem.*, **93**, 72-102 (2021).
13. S. Wang, Y. Bai, X. Yang, L. Liu, L. Li, Q. Lu, T. Li, T. Zhang, Highly stretchable potentiometric ion sensor based on surface strain redistributed fiber for sweat monitoring, *Talanta*, **214**, 120869 (2020).
14. M. Parrilla, R. Cánovas, I. Jeerapan, F. J. Andrade, and J. Wang, A Textile-Based Stretchable Multi-Ion Potentiometric Sensor, *Adv. Healthcare Mater.*, **5**, 996-1001 (2016).
15. H. J. Park, J. H. Yoon, K. G. Lee, and B. G. Choi, Potentiometric performance of flexible pH sensor based on polyaniline nanofiber arrays, *Nano Converg.*, **6**, 9 (2019).
16. C. Maccá, Response time of ion-selective electrodes Current usage versus IUPAC recommendations, *Anal. Chim. Acta*, **512**, 183-190 (2004).
17. J. M. Pingarrón, J. Labuda, J. Barek, C. M. A. Brett, M. F. Camões, M. Fojta, and D. B. Hibbert, Terminology of electrochemical methods of analysis (IUPAC Recommendations 2019), *Pure Appl. Chem.*, **92**, 641-694 (2020).
18. R. P. Buck, and E. Lindner, Recommendations for nomenclature of ion-selective electrodes (IUPAC Recommendations 1994), *Pure Appl. Chem.*, **66**, 2527-2536 (1994).
19. E. Bakker, E. Pretsch, and P. Bühlmann, Selectivity of Potentiometric Ion Sensors, *Anal. Chem.*, **72**, 1127-1133 (2000).

## Authors

- Seo Jin Kim; B.Sc., Graduate student, Department of Chemical Engineering, Kangwon National University, Gangwon-do 25913, Korea; qjatjr414356@gmail.com
- Seon Gyu Son; B.Sc., Graduate student, Department of Chemical Engineering, Kangwon National University, Gangwon-do 25913, Korea; tjrsrb84@gmail.com
- Jo Hee Yoon; M.Sc., Researcher, Department of Chemical Engineering, Kangwon National University, Gangwon-do 25913, South Korea; sefiraro@gmail.com
- Bong Gill Choi; Ph.D., Associate Professor, Department of Chemical Engineering, Kangwon National University, Gangwon-do 25913, Korea; bgchoi@kangwon.ac.kr